

Tin and zinc stable isotope characterisation of chondrites and implications for early Solar System evolution

J.B. Creech^{a,*}, F. Moynier^{b,c}

^a Department of Earth and Planetary Sciences, Macquarie University, NSW 2109, Australia

^b Institut de Physique du Globe de Paris, Université Sorbonne Paris Cité, Université Paris Diderot, 1 Rue Jussieu, Paris cedex 05 75328, France

^c Institut Universitaire de France, Paris, 75005, France

ARTICLE INFO

Editor: D. Porcelli

Keywords:

Tin

Stable isotopes

MC-ICP-MS

Double-spike

Volatile elements

ABSTRACT

Moderately volatile elements show variable depletion in terrestrial planets compared to the Sun. Isotopic ratios can be used as a signature of the processes at the origin of this depletion. Using a new method, the Sn stable isotope composition and elemental abundance in 36 primitive meteorites (chondrites) have been characterised to high precision. Significant mass-dependent Sn isotope variations are found within chondrites. The widest isotopic range is observed for the ordinary chondrites (-1.1‰ to $+0.5\text{‰}$ in $\delta^{122/118}\text{Sn}$, representing the difference in the $^{122}\text{Sn}/^{118}\text{Sn}$ ratio of the sample relative to our in-house standard, Sn_IPGP), with the ordinary chondrite groups extending to lighter isotopic compositions in the order $\text{H} > \text{L} > \text{LL}$, while carbonaceous and enstatite chondrites are heavier and occupy narrower compositional ranges. Tin and Zn isotope and concentration data are strongly correlated, particularly in ordinary chondrites, from which both sets of data were obtained on the same rock powders. Given the difference in geochemical behaviour (Zn lithophile/chalcophile and Sn chalcophile/siderophile) of these elements, this suggests that the primary control on the isotope and abundance variations is volatility. Chondrite groups show variability increasing with petrographic types, suggesting a secondary control from parent-body metamorphism. The isotopic composition of the bulk silicate Earth (BSE; $\delta^{122/118}\text{Sn} = 0.49 \pm 0.11\text{‰}$) overlaps with the carbonaceous chondrites ($\delta^{122/118}\text{Sn} = 0.43 \pm 0.12\text{‰}$; excl. CR and CK). Despite isotopic similarities for almost all isotopic systems, EH chondrites have Sn isotope compositions that are distinct from the bulk silicate Earth ($\delta^{122/118}\text{Sn} = 0.18 \pm 0.21\text{‰}$). Therefore, an enstatite chondrite-like bulk Earth requires that isotopically light Sn was lost from the silicate Earth, possibly into the metallic core or a sulphide matte, or by evaporative loss from Earth or its precursors.

1. Introduction

Chondrite meteorites contain the most primitive Solar System materials, and thus record information about the composition of the solar nebula and the accretion of and subsequent processing within asteroidal parent bodies. The CI group of carbonaceous chondrites is closest in composition to the solar photosphere, and thus is often taken to represent the composition of the solar nebula and the starting materials from which the planets could have formed. Volatile elements, that is, those elements with 50% condensation temperatures, T_c , between 250 K and 1250 K, exhibit widespread depletion relative to CI chondrites abundances in most meteorites and planetary materials, including the terrestrial planets. The depletions are broadly correlated with the T_c of the respective elements, and independent of their geochemical behaviour (e.g., Halliday and Porcelli, 2001; Palme et al.,

2014), suggesting that volatility processes played an important role. However, the origin of these depletions is debated, and may be a consequence of processes occurring during planetary accretion and/or inherited from prior fractionation in the solar nebula (e.g., Ringwood, 1966; O'Neill and Palme, 2008; Norris and Wood, 2017; Anders, 1968; Albarède, 2009).

Chondrites are undifferentiated meteorites that have not experienced sufficiently high temperatures to result in melting, and thus they have retained their primitive compositions, although they have undergone variable degrees of aqueous alteration (with the exception of enstatite chondrites) and thermal metamorphism (Scott and Krot, 2014; Brearley, 2014). The chondrites have relatively high volatile element abundances as compared with differentiated asteroidal parent bodies and the terrestrial planets, though these abundances vary between the chondrite groups (Wasson and Kallemeyn, 1988; Palme et al., 2014).

* Corresponding author.

E-mail address: john.creech@mq.edu.au (J.B. Creech).

<https://doi.org/10.1016/j.chemgeo.2019.02.028>

Received 3 October 2018; Received in revised form 13 February 2019; Accepted 16 February 2019

Available online 26 February 2019

0009-2541/ © 2019 The Authors. Published by Elsevier B.V. This is an open access article under the CC BY-NC-ND license

(<http://creativecommons.org/licenses/by-nc-nd/4.0/>).

Table 1
List of meteorite samples with Sn isotope and concentration results and literature data for Zn.

Sample	Group	Find/fall	Weathering grade	$\delta^{122/118}\text{Sn}$ (‰)	\pm (2 sd)	Total Sn in sample (μg)	[Sn] ($\mu\text{g g}^{-1}$)	$\delta^{66/64}\text{Zn}$ (‰)	\pm	[Zn] ($\mu\text{g g}^{-1}$)	Zn data source
Carbonaceous chondrites											
Jbilet Winselwan	CM2	Find (Northwest Africa)		0.304	0.076	0.33	1.05	0.38	0.04	172	a [†]
LON 94101	CM2	Find (Antarctica)	Be	0.532	0.123	0.30	0.95	0.37	0.04	184	a
Murchison	CM2	Fall		0.496	0.354	0.45	1.46	0.40	0.06	186	a [§]
Murray	CM2	Fall		0.610	0.031	0.40	0.81	0.37	0.02	187	a [§]
Tagish Lake	C2-ung	Fall		0.517	0.221	0.42	1.17	0.45	0.06	217	b
DOM 10101	CO3	Find (Antarctica)	Be	0.279	0.024	0.16	0.53	0.17	0.11	102	a [†]
MIL 090010	CO3	Find (Antarctica)	A/B	0.616	0.034	0.23	0.56	0.17	0.11	102	a [†]
Allende	CV3	Fall		0.499	0.111	0.19	0.63	0.29	0.04	172	a [§]
LAP 02206	CV3	Find (Antarctica)	B	0.365	0.025	0.19	0.63	0.24	0.12	110	a [†]
MIL 090001	CR	Find (Antarctica)	B	0.752	0.036	0.12	0.41				
LEW 87009	CK	Find (Antarctica)	Ae	1.242	0.070	0.14	0.48				
Enstatite chondrites											
SAH 97096	EH3	Find (Northwest Africa)		0.349	0.044	0.42	1.43	0.31	0.09	309	c
GRO 99517	EH3	Find (Antarctica)	C	0.071	0.084	0.54	1.53	0.31	0.09	309	c [†]
LAR 06252	EH3	Find (Antarctica)	Be	0.193	0.118	0.70	1.58	0.31	0.09	309	c [†]
MIL 07028	EH3	Find (Antarctica)	B	0.144	0.044	0.99	2.17	0.31	0.09	309	c [†]
Indarch	EH4	Fall		0.149	0.028	0.69	1.65	0.21	0.10	280	c [§]
MAC 02837	EL3	Find (Antarctica)	C	-0.217	0.103	0.58	1.13	0.12	0.12		c [†]
MAC 02747	EL4	Find (Antarctica)	B/C	-0.295	0.042	0.71	1.17	0.12	0.12		c [†]
NW Forrest	EL6	Find (Australia)		0.580	0.141	0.51	0.90	7.35	0.09		c
Ordinary chondrites											
Clovis (no. 1)	H3.6	Find (USA)		-0.632	0.023	0.09	0.44	-2.32	0.09		a
Grady (1937)	H3.7	Find (USA)		0.002	0.011	0.23	0.50	0.98	0.09	35	d*
QUE 99018	H4	Find (Antarctica)	A/B	-0.004	0.039	0.24	0.32	-0.03	0.09	81	d*
Agen	H5	Fall		0.543	0.034	0.93	1.12	0.70	0.09	32	d*
LAR 06392	H5	Find (Antarctica)	A/B	-0.615	0.014	0.16	0.45	-0.72	0.09	44	d*
ALH 90411	L3.7	Find (Antarctica)	Be	-0.697	0.026	0.12	0.35	-0.75	0.09		a
ALHA77215	L3.8	Find (Antarctica)	B	-0.017	0.023	0.29	0.43	-0.28	0.09	43	d*
Barratta	L4	Find (Australia)		-0.308	0.033	0.11	0.42	-1.03	0.09	55	d*
ALH 85033	L4	Find (Antarctica)	A	-1.013	0.232	0.17	0.40	-1.31	0.09	43	d*
MAC 87302	L4	Find (Antarctica)	A/B	-0.125	0.020	0.15	0.38				
GRO 95540	L5	Find (Antarctica)	A	0.126	0.021	0.19	0.38	0.71	0.09	63	d*
ALH 84126	LL3.4	Find (Antarctica)	B	-0.315	0.184	0.05	0.20	0.53	0.09	102	d*
DAV 92302	LL3.6	Find (Antarctica)	B	-0.710	0.122	0.14	0.37	-0.67	0.09	108	d*
LAP 02266	LL4	Find (Antarctica)	A	0.067	0.046	0.13	0.44	-0.38	0.09	50	d*
Saint-Séverin	LL6	Fall		-0.290	0.130	0.33	0.50	-0.40	0.09	47	b
LAR 06250	LL6	Find (Antarctica)	A/B	0.062	0.028	0.18	0.33	0.26	0.09	39	d*
Y-791067	LL7	Find (Antarctica)	A	-1.080	0.246	0.10	0.36	-2.06	0.09	47	d*

Weathering grades are from the NASA meteorite working group (MWG) and use the classification scheme of Wlotzka (1993). Zn data sources: ^aPringle et al. (2017), ^bLuck et al. (2005), ^cMoynier et al. (2011), ^dPaniello (2013).

[†] Group mean.

[§] Sample mean.

* Sn analyses used same sample powders as Zn data.

The carbonaceous chondrite classes show a volatile depletion trend in the order CI-CM-(CO, CV)-CK (Palme et al., 2014). Compared with carbonaceous chondrites, the abundances of moderately volatile elements, such as Zn or Sn, are lower in ordinary chondrites, while some are relatively enriched in enstatite chondrites (Palme et al., 2014).

The volatile element histories of Earth and other planetary materials have been extensively discussed and debated in the literature. Hypotheses to explain the volatile element depletions include incomplete condensation from solar nebula (Wasson and Chou, 1974; Albarède, 2009), volatile loss by evaporation during accretion (Ringwood, 1966; Tyburczy et al., 1986; O'Neill and Palme, 2008; Hin et al., 2017; Norris and Wood, 2017), or mixing of distinct volatile rich and volatile poor primordial reservoirs (Larimer and Anders, 1967; Clayton and Mayeda, 1999; Luck et al., 2003; Pringle et al., 2017). Isotopes are known to fractionate during kinetic and equilibrium processes related to vaporisation/condensation, and thus isotopic variations of moderately volatile elements may help to identify signatures relating to such processes. Several recent studies of stable isotopes of moderately volatile elements (e.g., K, Cl, Zn, Cu, Ga, Rb, Cd, Se) have revealed isotopic fractionation due to volatile loss during formation and evolution of the Moon (Poitrasson et al., 2004; Schediwy et al., 2006; Sharp et al., 2010; Kato et al., 2015; Boyce et al., 2015; Kato and

Moynier, 2017a; Wang and Jacobsen, 2016; Sossi et al., 2018), identified source reservoirs for components of chondrites (Luck et al., 2005, 2003; Wombacher et al., 2008; Moynier et al., 2011; Pringle et al., 2017), and indicated volatile loss driven by impacts on planetesimals (Pringle et al., 2014; Pringle and Moynier, 2017; Hin et al., 2017).

While significant attention has been given recently on using the stable isotopic composition of moderately volatile elements as a signature of the processes at the origin of the volatile depletion, most elements that have been studied were lithophile. With a T_c of 704 K (Lodders, 2003), Sn is more volatile than most of the elements mentioned above. Being that Sn is also moderately chalcophile and siderophile, the distribution of Sn in Solar System materials may also trace other planetary processes, such as core formation or sulphide segregation. The abundance of Sn in the silicate Earth, which is depleted by a factor of 33 (Jochum et al., 1993) relative to CI chondrites, may thus be a consequence of either depletion of volatiles in Earth's precursor materials or from the primordial Earth, removal of Sn into metals or sulphides during planetary differentiation, or a combination of these. Tin stable isotope data may reveal isotopic signatures of these different processes, and provide insights into this critical period in our planet's history.

Despite the potential of Sn as a tracer of early Solar System

processes, there are relatively few Sn elemental or isotopic data for meteoritic samples in the literature. Tin concentration data have been published for a number of chondrites (Shima, 1964; Hamaguchi et al., 1969; de Laeter et al., 1974; Wasson and Kallemeyn, 1988; Friedrich et al., 2002, 2003; Barrat et al., 2012; Friedrich et al., 2014), achondrites (Mittlefehldt and Lindstrom, 1991; Morgan et al., 1978) and iron meteorites (de Laeter and Jeffery, 1965, 1967). However, Sn isotope data for extraterrestrial materials in the literature are so far limited to a handful of iron meteorites (de Laeter and Jeffery, 1965, 1967) and acid leachates from Allende (Loss et al., 1990) and with analytical uncertainties on the order of $\sim 1\text{--}2\%$ per atomic mass unit (amu). We have recently developed a new method based on double-spike addition and multi-collection inductively-coupled-plasma mass spectrometry (MC-ICPMS) that allowed us to improve the analytical uncertainty by a factor of > 20 compared to those previous works (Creech et al., 2017; Badullovich et al., 2017).

Here, we present Sn stable isotope data for a suite of 36 chondrite meteorites, representing all major chondrite groups and a broad range of compositions and metamorphic grades. Zinc and tin isotope and concentration data for ordinary chondrites were acquired on the same sample powders, allowing a direct comparison between these isotope systems. Based on these data, we make inferences about the nature of the building blocks that accreted to form Earth, and the origins of Earth's budget of moderately volatile elements.

2. Materials and methods

2.1. Samples

A total of 36 bulk chondrite samples were analysed in this study, and sample names and information are summarised in Table 1. Twelve of the samples analysed are carbonaceous chondrites, comprising four CM, two each of CO and CV, one specimen each of CK and CR, and one ungrouped C2 chondrite. Of the eight enstatite chondrites analysed, five are EH and three are EL. The 17 ordinary chondrites comprise five H chondrites, six L chondrites and six LL chondrites. The ordinary chondrites span a range of petrologic types, as indicated in Table 1. Of the chondrite samples, seven were observed falls, while the remaining 29 are finds from Antarctica (23), Australia (2), Northwest Africa (2) or the USA (2). Zinc isotope and concentration data from the literature are included in the last columns of Table 1, with the sources given below; for many samples, the Zn data were obtained on the same sample powders as the Sn data presented here, and were previously published in a PhD thesis (Paniello, 2013), following the same methods as Paniello et al. (2012). Full data for all replicates are also available in the Supplementary Information.

2.2. Chemicals and standard solutions

All laboratory work was performed in a class-100 clean room environment at the Institut de Physique du Globe de Paris, France. Pre-cleaned Savillex Teflon PFA beakers were used for all samples and solutions processed in this study. BASF Selectipur® AR grade acids (69% HNO₃, 37% HCl) were further purified by sub-boiling distillation using Savillex DST-1000 distillation units. All dilutions were carried out using ultra-pure (18.2 M Ω cm) Milli-Q water.

The Sn_IPGP standard described by Creech et al. (2017) was used as an isotope reference, and remains available to other laboratories on request.

2.3. Sample preparation and dissolution

Samples comprising 250–500 mg of rock powder were digested in a mixture of concentrated HF:HNO₃ in closed teflon beakers on a hotplate at 120 °C. After dissolution, samples were dried down at 100 °C and the residue taken up in aqua regia and refluxed overnight at 120–150 °C to

destroy any fluoride complexes that may have formed during the digestion. Afterwards, samples were dried down at 100 °C, and the samples were then evaporated to dryness in 10 M HCl before finally bringing into solution in 2 mL of 0.5 M HCl for anion-exchange chemistry.

Samples were double-spiked with a ¹¹⁷Sn–¹²²Sn double-spike prior to digestion by adding the double-spike directly to the sample beaker. Double-spike amounts were calculated based on approximate Sn content of samples, and designed to give optimal proportions of approximately 39.8% Sn from the double-spike and 60.2% from the sample as detailed by Creech et al. (2017).

2.4. Chemical separation of Sn

Chemical separation of Sn was performed using Eichrom TRU resin as described by Creech et al. (2017). Biorad columns were prepared with 1.5 mL per column of TRU resin and cleaned prior to sample loading with alternating reservoir volumes of acids (0.5 M HCl, 2 × 0.5 M HNO₃) and H₂O. Samples were loaded on the columns in 2 mL of 0.5 M HCl, and subsequently rinsed with 5 mL of 0.5 M HCl and 7 mL of 0.25 M HCl. Tin cuts were collected in 10 mL of 0.5 M HNO₃. Replicate analyses of selected samples were made to determine the reproducibility of the method, as discussed in Section 3.1. In addition, for comparison, splits of three samples (Jbilet Winselwan (CM2), Allende (CV3) and SAH 97096 (EH3)) were processed through the alternative chemistry proposed by Wang et al. (2017), which employs anion exchange resin (AG1-X8) in a three-pass chemistry, as opposed to our two-pass chemistry in TRU resin.

2.5. Mass spectrometry and data reduction

Tin stable isotope measurements were carried out using a Thermo-Scientific Neptune Plus MC-ICPMS at the Institut de Physique du Globe de Paris, France under the same operating conditions as described by Creech et al. (2017). Sample and standard solutions were prepared for isotope measurements with Sn concentrations of typically 100 ng mL⁻¹ in 0.5 M HCl. Solutions were introduced into the mass spectrometer using an ESI Apex-IR desolvator and a PFA nebuliser with an uptake rate of ca. 100 μ L min⁻¹. The Neptune was run in low resolution mode, with a mass resolution of ~ 1800 . Ion beams at ¹¹⁷Sn, ¹¹⁸Sn, ¹¹⁹Sn, ¹²⁰Sn, ¹²¹Sb, ¹²²Sn, ¹²³Sb, ¹²⁴Sn and ¹²⁵Te were simultaneously collected in a single cycle using Faraday cups, with all Sn channels plus ¹²⁵Te connected to amplifiers with 10¹¹ Ω resistors and both Sb channels using amplifiers with 10¹² Ω resistors. This configuration yields a sensitivity of ~ 600 V ppm⁻¹ of Sn. Faraday collector gains were calibrated prior to the beginning of each analytical session, and baselines were measured on-peak for a duration of 14 min between every analysis, with the last ca. 120 s being subtracted from the subsequent analysis. Analyses of samples had a duration of 412 s, corresponding to a total of ca. 70 ng of Sn consumed per analysis under normal conditions.

Data reduction was conducted offline using the freely available double-spike data reduction tool *IsoSpike* (www.isospike.org; Creech and Paul, 2015). Isotope results are reported in $\delta^{122/118}\text{Sn}$ notation, which reports the per mil (‰) difference in the ¹²²Sn/¹¹⁸Sn ratio relative to Sn_IPGP, our in-house Sn isotope standard.

In our previous work, we demonstrated that the external reproducibility of this method is ca. $\pm 0.065\%$ (2 sd) on the $\delta^{122/118}\text{Sn}$ ratio, or ca. $\pm 0.016\%$ per amu, based on 10 analyses of replicate digestions of BHVO-2 and BCR-2 (Creech et al., 2017). The reproducibility for chondrite samples is examined in Section 3.1. In all figures, error bars reflect the 2 sd of all analyses included in the data point or the uncertainty of the method, whichever is larger.

Table 2
Sn isotope data for samples processed in replicate, with one replicate of each being processed using the alternative chemistry of Wang et al. (2017).

Sample	Group	$\delta^{122/118}\text{Sn}$	\pm (2 sd)	Total Sn in sample (μg)	Sn conc. ($\mu\text{g g}^{-1}$)
Jbilet Winselwan	CM2	0.252	0.029	0.333	1.054
Replicate		0.274	0.023	0.623	1.153
Replicate		0.338	0.027	0.739	1.176
Replicate		0.288	0.017	0.585	1.083
Replicate		0.323	0.015	0.681	1.084
Average		0.295	0.071		
Alternative chemistry replicate		0.348	0.018	0.533	0.987
Allende	CV3	0.573	0.019	0.612	0.646
Replicate		0.503	0.016	0.667	0.636
Replicate		0.465	0.020	0.623	0.680
Average		0.514	0.110		
Alternative chemistry replicate		0.526	0.013	0.616	0.651
SAH 97096	EH3	0.368	0.021	0.424	1.428
Replicate		0.359	0.011	0.732	1.193
Replicate		0.334	0.022	0.555	1.262
Replicate		0.339	0.020	0.733	1.194
Replicate		0.318	0.030	0.557	1.266
Average		0.344	0.040		
Alternative chemistry replicate		0.375	0.011	0.738	1.202

3. Results

3.1. Reproducibility and chemistry comparison

To both determine the reproducibility of our method when applied to chondrite samples and test the consistency of our chemical method with the recently published method of Wang et al. (2017), we analysed three samples—Jbilet Winselwan (CM2), Allende (CV3) and SAH 97096 (EH3)—in several replicate digestions, including aliquots of one replicate of each sample taken prior to chemistry and processed using the Sn purification procedure described by Wang et al. (2017). The results of these replicate analyses and the comparison with those processed using the alternative chemistry are presented in Table 2 and Fig. 3.

Replicates of the three chondrite samples Jbilet Winselwan (CM2), Allende (CV3) and SAH 97096 (EH3), were found to have measurement repeatability on $\delta^{122/118}\text{Sn}$ of $\pm 0.071\text{‰}$, $\pm 0.110\text{‰}$ and $\pm 0.040\text{‰}$, respectively (Table 2; Fig. 3). Both of the carbonaceous chondrites samples were found to have slightly poorer reproducibility than that previously estimated for our method based on replicates of the USGS basaltic reference materials BHVO-2 and BCR-2 of $\pm 0.065\text{‰}$ on the same ratio. This could reflect true isotopic variability in those samples and over- or under-sampling of different phases; future analyses should test using larger sample masses. The enstatite chondrite data, on the other hand, were very reproducible, partly owing to the relatively high abundance of Sn in EH chondrites as compared with the other chondrite groups.

The replicates that were passed through the alternative chemical purification described by Wang et al. (2017) reproduce very well the values determined using our chemical method (Table 2; Fig. 3). Thus, no significant isotopic variability is likely to be attributable to the use of either of these methods, in this or future data, so long as a double-spike approach is used.

3.2. Tin isotope and abundance variations in chondrites

Significant Sn isotopic variation was observed between the chondrite groups, with $\delta^{122/118}\text{Sn}$ compositions spanning a range of $> 2\text{‰}$ (Table 1, Figs. 1–4).

The carbonaceous chondrites all together have an error weighted

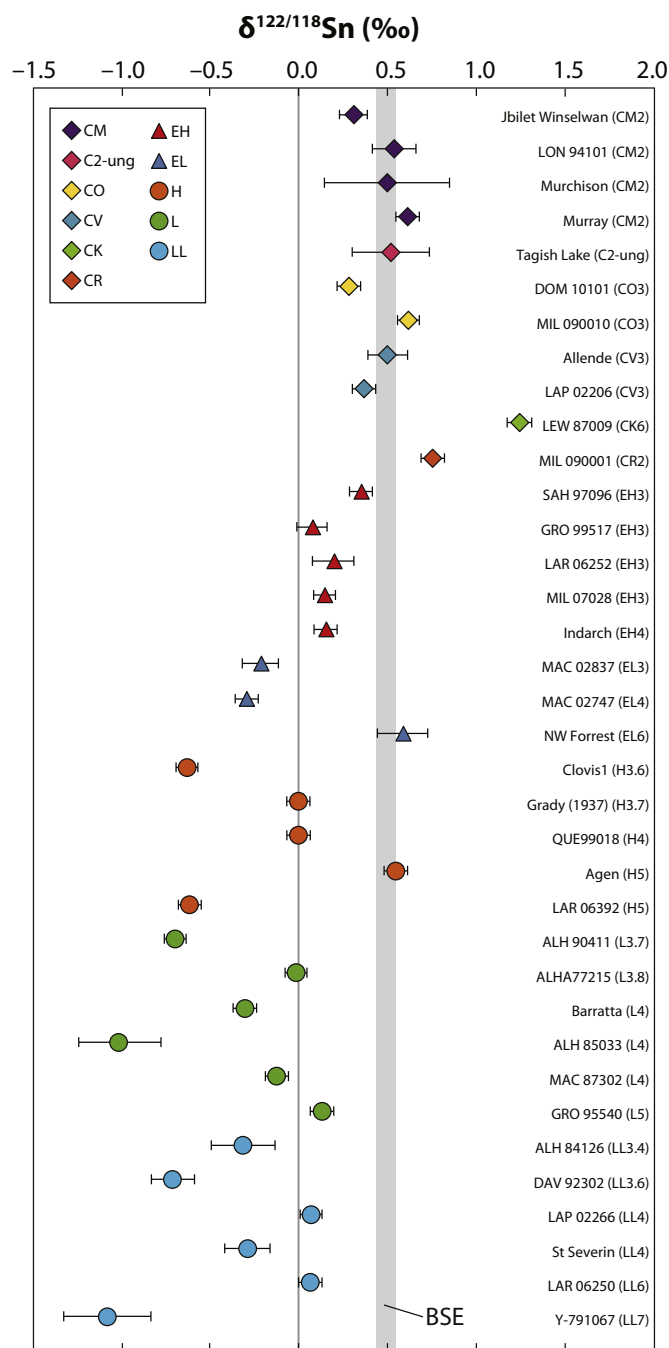


Fig. 1. Sn isotope data for all chondrite samples. Error bars reflect the 2 sd of all analyses included in the data point or the uncertainty of the method, whichever is larger. The shaded box represents the bulk silicate Earth composition of Badullovich et al. (2017).

mean composition of $\delta^{122/118}\text{Sn} = 0.49 \pm 0.15\text{‰}$ (95% CI). If the CR and CK samples are excluded, as both represent single specimens and fall outside of the range of the other chondrite groups, the mean composition becomes narrower at $\delta^{122/118}\text{Sn} = 0.43 \pm 0.12\text{‰}$.

The enstatite chondrites have distinctly different isotopic compositions between the EL and EH groups. The EH chondrites are all isotopically similar, and with the exception of SAH 97096, all plot within error of one another, with SAH 97096 slightly outside this grouping (Fig. 1). The EH chondrites have a mean $\delta^{122/118}\text{Sn} = 0.18 \pm 0.21\text{‰}$. Of the three EL chondrites analysed, two (MAC 02837 and MAC 02747) are identical within uncertainties, while the third (Northwest Forrest) is markedly different. That specimen is also an extreme outlier in Zn

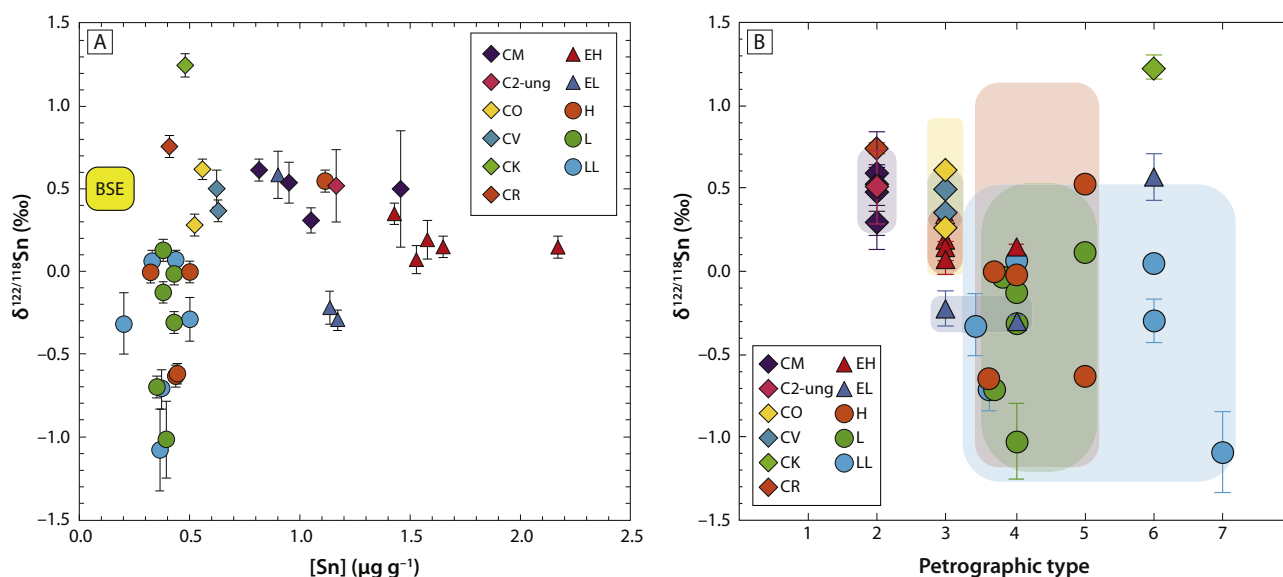


Fig. 2. A) Sn isotopes vs. concentration for all chondrite meteorite samples. Also indicated is the estimated composition of the bulk silicate Earth (BSE) from Badullovich et al. (2017). B) Tin isotope composition versus petrographic type. Shaded regions indicate the 2 sd (vertical axis) and range of petrographic types within the groups of the corresponding colour, and are only shown for groups with multiple specimens analysed (the EL6 chondrite Northwest Forrest is excluded from the group mean as described in the text). (For interpretation of the references to colour in this figure legend, the reader is referred to the web version of this article.)

isotopes, recording one of the heaviest Zn isotopic compositions in Solar System materials (Moynier et al., 2011). Excluding Northwest Forrest as an outlier, the EL chondrites have a composition of $\delta^{122/118}\text{Sn} = -0.26 \pm 0.11$ ‰, yielding a mean enstatite chondrite composition of $\delta^{122/118}\text{Sn} = 0.06 \pm 0.42$ ‰.

The ordinary chondrites have the largest range in isotopic compositions, extending from ca. +0.5 ‰ to -1.0 ‰ (Fig. 1). These isotopic variations do not appear to correlate with Sn depletions in these samples, but rather, the ordinary chondrites have a relatively narrow range in Sn content (Fig. 2A), similar to the pattern observed for Ga by Kato and Moynier (2017b). The Sn isotope data do not strongly correlate with petrologic types (i.e., metamorphic grade, aqueous alteration), although increased scatter is apparent in groups with higher petrologic

types (5–7; Fig. 2B), as discussed further in Section 4.1.

In chondrite samples for which literature data are available, our measured Sn abundances in our chondrite samples are generally in good agreement with previously reported values (see Supplementary Information); where our concentrations differ, since the precision of our technique is considerably higher than the older techniques by which the reference values were obtained, we rely on the quality of our concentrations.

4. Discussion

4.1. Limited effect of petrologic types

The EH samples analysed show no significant correlation with metamorphic grade; the isotopically heaviest enstatite chondrite (SAH 97096; $\delta^{122/118}\text{Sn} = 0.349 \pm 0.044$ ‰) is an EH3, while Indarch, the only higher grade EH sample (EH4) has a $\delta^{122/118}\text{Sn} = 0.149 \pm 0.028$ ‰, which is intermediate amongst the EH3 data. However, a difference is apparent in the EL chondrite data. The EL3 and EL4 samples are similar, whereas the single EL6 sample has the heaviest isotopic composition of all of the enstatite chondrites (Table 1; Fig. 1). The EL6 sample also has lower [Sn] than EL3–4 chondrites, although not significantly so (0.90 vs. 1.12 and 1.17 $\mu\text{g g}^{-1}$, respectively; Table 1). The large isotopic difference between the EL3–4 and EL6 samples could indicate that the Sn isotope composition has been modified through thermal metamorphism, although without significantly affecting [Sn] abundance (Table 1). EL6 samples are highly enriched in the heavier isotopes of Zn (Moynier et al., 2011; see data in Table 1), which has been attributed to preferential evaporation of the lightest isotopes of Zn during thermal metamorphism at the surface of the EL chondrite parent body. The isotopic fractionation of Zn in EL6 is much larger than for Sn (by almost a factor 10 on a per amu basis). Moynier et al. (2011) showed that Zn was mostly carried by silicate phases in the EL6 Blithfield (~70% in silicate vs. 30% in sulphides) and that the silicates were much more enriched in the heavier isotopes of Zn compared to the sulphides ($\delta^{66/64}\text{Zn} = 6.99$ ‰ in silicate vs. 2.07 ‰ in sulphides). The origin for the limited isotopic fractionation in the sulphides was not discussed in Moynier et al. (2011), but are likely related to the difference of speciation between the melt and the gas during the evaporation,

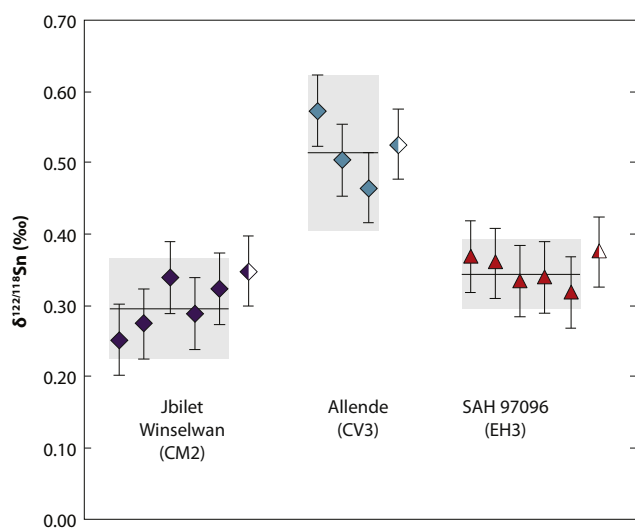


Fig. 3. Replicate measurements of three meteorite samples (filled symbols) showing the measurement repeatability, and the comparison of data (half-filled symbols) for samples purified using the alternative chemistry (see text). Lines and grey boxes represent the mean and 2 sd of the data they enclose. Error bars reflect the 2 sd of all analyses included in the data point or the uncertainty of the method, whichever is larger.

which would be dependent on the composition of the melt. Tin is more chalcophile than Zn (at least under more oxidising conditions; Patten et al., 2013), and while we did not do phase separation for Sn, it can be inferred that the large majority of Sn in the EL6 would be carried by the sulphides, which may be the reason for the difference of isotopic behaviour between Zn and Sn during thermal metamorphism on the EL parent body. Similar behaviour is also observed for two other highly chalcophile elements (S and Se), which show limited isotopic fractionation between metamorphic grades in enstatite chondrites (Defouilloy et al., 2016; Vollstaedt et al., 2016). Alternatively, the difference in behaviour could be related to the more siderophile nature of Sn versus the lithophile behaviour of Zn.

Ordinary chondrites, show no strong correlation between Sn isotopic compositions and metamorphic grades. The equilibrated and un-equilibrated ordinary chondrites completely overlap. The most metamorphosed sample, Y-791067, is identified as an LL7, and thus has been metamorphosed to nearly the point of melting, and that sample does have the lightest Sn isotope composition of any sample analysed so far. However, the lack of a coherent trend within the rest of the ordinary chondrites suggests that Sn isotopes are, at most, variably affected by metamorphism. While isotopic compositions do not strongly correlate with petrologic type for individual meteorite specimens, we do however observe an increase in the scatter in isotope data for group with higher petrologic type (Fig. 2B). This indicates that metamorphism likely exerts a secondary control on the isotopic composition of chondrite meteorites, leading to this enhanced variability. Similar isotopic behaviour is observed for S (Gao and Thiemens, 1991) and for Se (Vollstaedt et al., 2016), which is also isotopically homogeneous between ordinary chondrites groups while its abundance is variable.

The carbonaceous chondrites all show varying degrees of aqueous alteration (Brearley, 2014; Palme et al., 2014). The CM chondrites have experienced the highest degree of aqueous alteration of the carbonaceous chondrites analysed here. Despite the strong alteration in that group, the CMs do not exhibit significantly greater Sn isotope variability than the other chondrite groups (Fig. 2B), and the means of the three carbonaceous chondrite groups for which we have multiple specimens overlap within uncertainties. The CM chondrites do, however, have higher Sn abundances as compared with the other carbonaceous chondrites, although given that the CO and CV chondrites have also undergone varying degrees of aqueous alteration (Brearley, 2014), the higher Sn abundances cannot be readily attributed to alteration effects. Rather, these are likely a primary characteristic of the CM chondrites, and the Sn abundances are consistent with previous observations for Sn, and other moderately volatile elements generally, in chondrites (e.g., Wasson and Kallemeyn, 1988; Palme et al., 2014).

We also note that there is so far no indication of any effect of terrestrial weathering on Sn isotopic compositions or Sn content. This is supported by the extensive data set of by Braukmüller et al. (2018), which has samples from all major chondrite groups and includes hot- and cold-desert finds as well as falls. These data show no resolvable enrichments or depletion in [Sn], irrespective of the terrestrial exposure. Furthermore, plotting Sn content versus a fluid mobile/immobile element pair (e.g., Ba/Yb; Fig. S1) shows no systematic differences between finds and falls, suggesting terrestrial weathering does not significantly affect Sn. Fig. S1 does suggest that Jbilet Winselwan is the sample most likely to be affected by terrestrial weathering, although that sample does not have a clearly distinct Sn isotopic composition. For all groups where specimens have been analysed from both finds and observed falls, no systematic or significant differences were identified in the Sn isotope data between the hot or cold desert finds and falls, when compared with the scatter in those groups.

4.2. Origin of Sn and Zn isotopic variations in chondrites

Tin and Zn abundances in the various chondrite groups are strongly correlated ($R^2 = 0.85$; Fig. 4A). For both elements, the enstatite

chondrites have the highest concentrations of the samples analysed, while the ordinary chondrites are the most depleted, and carbonaceous chondrites span a range intermediate between the other groups. A similar correlation is also true for isotopes of Sn and Zn (Fig. 4B) in ordinary chondrites ($R^2 = 0.62$; Fig. 4B), with the lightest samples and heaviest samples being common between both isotope systems. Due to the lack of common Zn isotope data for individual carbonaceous chondrites or enstatite chondrites, no meaningful correlations can be inferred for those groups, although both groups lie close to the isotopically heavy end of the trend observed in ordinary chondrites. Neither isotope system correlates with the degree of elemental depletion, nor with other parameters such as metamorphic grade.

Taking into account the similar relative mass differences in the ratios (ca. 3.2% for $^{122}\text{Sn}/^{118}\text{Sn}$, ca. 3.0% for $^{66}\text{Zn}/^{64}\text{Zn}$), the magnitude of isotope fractionation of Zn in the ordinary chondrite samples is approximately double than that of Sn. Since Zn and Sn have different geochemical behaviour (Zn is lithophile/chalcophile and Sn chalcophile/siderophile), the strong correlation between the $\delta^{66/64}\text{Zn}$ and $\delta^{122/118}\text{Sn}$ between ordinary chondrites would suggest that the isotopic variability for both elements is controlled by volatility. Chondrules are the main component of ordinary chondrites (60–80% of the total mass) and are thought to be formed during high temperature processes under conditions of rapid heating and cooling (e.g., Jones, 2012) during a ~ 4 Myr period starting with the formation of the calcium-aluminium rich inclusions (CAI; Bollard et al., 2017). Individual chondrules from the CV chondrite Allende (Pringle et al., 2017) and the ordinary chondrite NWA 5687 (Bollard et al., 2017) are variably enriched in the light isotopes of Zn. The origin of this light isotope enrichment was proposed to be controlled by the separation between isotopically heavy silicates and isotopically light sulphides either during ejection or evaporation of sulphides from chondrules or their precursors (Pringle et al., 2017), following models from Uesugi et al. (2010) and Wasson and Rubin (2010). Similar light isotope enrichment in chondrules has also been suggested for other moderately volatile elements such as Rb (Pringle and Moynier, 2017), Cd (Wombacher et al., 2008), and Ag (Schönbächler et al., 2008). While no data on the Sn isotopic composition of individual chondrules are presently available, the enrichment in light isotopes observed in ordinary chondrites and the correlation between $\delta^{66/64}\text{Zn}$ and $\delta^{122/118}\text{Sn}$ suggest that chondrules would also be isotopically light in Sn, and would control the isotopically light composition of the bulk ordinary chondrites.

In a recent abstract, Bourdon et al. (2017) reported similar light Sn isotope enrichment in bulk ordinary chondrites, and proposed an alternative mechanism for the light isotope enrichment to be controlled by kinetic effects during condensation. Schönbächler et al. (2008) and Wombacher et al. (2008) also suggested that the light isotope enrichment of Ag and Cd in ordinary chondrites were produced by evaporation/condensation and open system metamorphism on the ordinary chondrite parent body. Such models would predict a correlation between the $\delta^{122/118}\text{Sn}$ and the Sn concentration, which is presently unclear (Fig. 2A). However, the exact behaviour of Sn during evaporation and condensation processes (both kinetic or under equilibrium) is presently unknown, and more analytical, experimental and theoretical work will need to be done in the future.

4.3. Parent bodies of enstatite chondrites

The enstatite chondrites formed in extremely reducing conditions, and are amongst the most reduced rocks in the Solar System (e.g., Sears et al., 1982). Enstatite chondrites plot on the terrestrial fractionation line (TFL) for O isotopes, close to the composition of the Earth/Moon (Clayton et al., 1984). The origin of the variety of enstatite chondrites is debated (Keil, 1989). Some have suggested that the EL and EH chondrites may have formed on a single, stratified parent body (e.g., Biswas et al., 1980; Kong et al., 1997), while others argue that these are derived from at least two separate parent bodies (e.g., Baedeker and

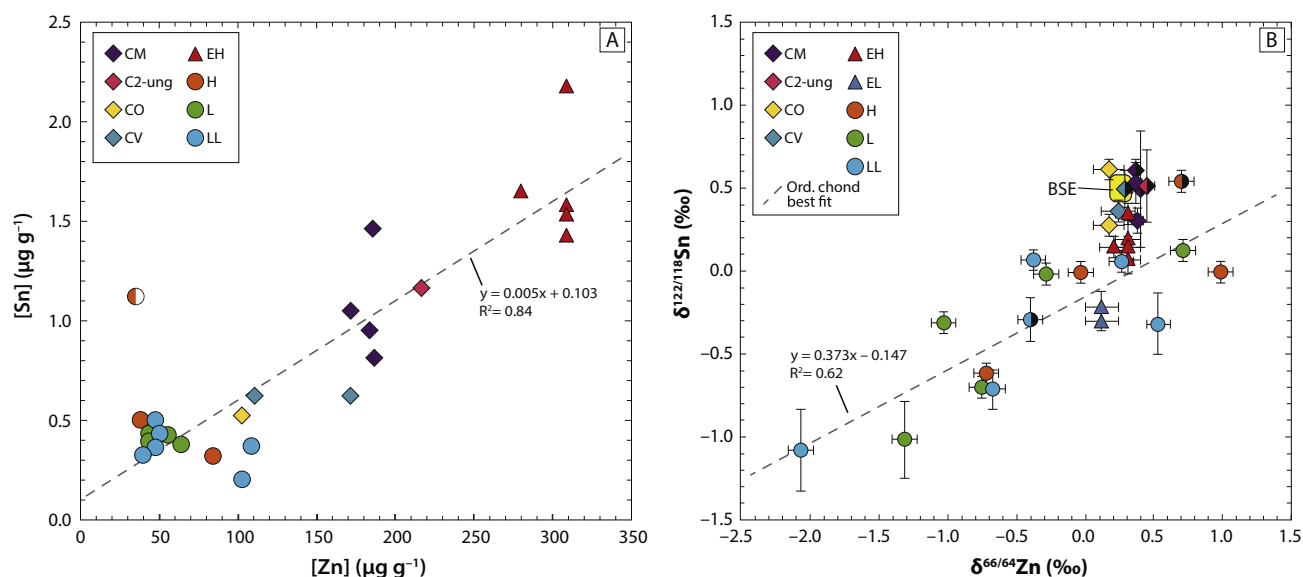


Fig. 4. A) Sn and Zn elemental abundances in chondrites, with a best fit line showing the correlation between [Sn] and [Zn] for all chondrite groups. The half-filled symbol represents the H5 chondrite Ager; excluding this sample from the regression has very little impact on the slope or intercept, but does reduce the R^2 value from 0.84 to 0.75. B) Sn and Zn isotope variations in chondrites. The best fit line plotted is a regression through only ordinary chondrite data, where the Sn and Zn data were acquired from the same sample powders. The yellow box indicated represents the composition of the bulk silicate Earth (BSE) for both isotope systems; Sn and Zn BSE compositions are from [Badullovich et al. \(2017\)](#) and [Chen et al. \(2013\)](#), respectively. Half-filled symbols represent meteorite specimens that are observed falls. (For interpretation of the references to colour in this figure legend, the reader is referred to the web version of this article.)

[Wasson, 1975](#); [Keil, 1989](#); [Lin and Goresy, 2002](#)). Tin stable isotope data provide some additional constraints to test these different hypothesised scenarios.

The EH chondrites are relatively enriched in some moderately volatiles, such as Zn ([Palme et al., 2014](#)), while the EL chondrites are more depleted. The same holds true for Sn in our data set. The EH chondrites and EL3–4 chondrites have distinctly (i.e., ca. 0.4 ‰) different Sn isotope compositions, with the EH samples having, on average, ca. 40% higher [Sn] than the EL group. No process has yet been identified that would lead to both heavier $\delta^{122/118}\text{Sn}$ and increased Sn concentrations. On Earth, igneous processes have been shown to fractionate Sn isotopes, as well as have strong controls on the elemental abundance of Sn ([Creech et al., 2017](#); [Badullovich et al., 2017](#); [Wang et al., 2018](#)), although in those terrestrial settings, the sense of the fractionation is the opposite of that observed between EH and EL chondrites, with more evolved rocks having higher [Sn] but lighter $\delta^{122/118}\text{Sn}$. However, terrestrial analogues may not be applicable due to the vastly different (i.e., extremely reducing) redox conditions under which the enstatite chondrites formed. Therefore, it is difficult to reconcile our observations for enstatite chondrites with contemporaneous layers coexisting on a single parent body. It may be possible to reconcile this scenario if the variations were a consequence of time rather than parent-body processes, with the two end members reflecting different nebular compositions at different times. A similar hypothesis was proposed recently to explain Ca isotope variations amongst terrestrial planetary bodies ([Schiller et al., 2018](#)). This hypothesis could be tested by analysing Sn isotope ratios for additional terrestrial bodies (e.g., Moon, Mars, Vesta). At the present time, the most likely interpretation of Sn isotope data is that EL and EH chondrites represent separate parent bodies, and that these parent bodies sampled Sn reservoirs with different isotopic compositions arising from their location or accretion times within the solar nebula.

4.4. Tin isotope constraints on Earth's building blocks

[Badullovich et al. \(2017\)](#) estimated the bulk silicate Earth (BSE) Sn isotope composition based on analyses of komatiites and basalts as $\delta^{122/118}\text{Sn} = 0.49 \pm 0.11$ ‰, with more evolved igneous rocks tending

towards lighter isotopic compositions due to fractional crystallisation. Here, the variations amongst the chondrites are explored in the context of the BSE composition.

The carbonaceous chondrites analysed here broadly overlap in $\delta^{122/118}\text{Sn}$ with the BSE estimate, although some samples extend to both lighter and heavier isotopic compositions (Fig. 2A). This is also true for Zn, with the BSE composition falling within the range for carbonaceous chondrites for both isotope systems (Fig. 4B). The ordinary chondrites, with one exception, all have isotopic compositions very much lighter than the BSE value. Given the isotopic similarities between Earth and enstatite chondrites for most isotope systems (e.g., [Clayton et al., 1984](#); [Javoy, 1995](#); [Trinquier et al., 2007](#); [Regelous et al., 2008](#); [Mougel et al., 2017](#)), most interesting perhaps is the offset between the BSE value and enstatite chondrites. All of the enstatite chondrite samples analysed for Sn isotopes so far are lighter than the BSE, with only one EH sample being within error of BSE. The higher-Sn EH chondrites are closer to, but still lighter than, BSE, and the lower-Sn EL chondrites are significantly lighter than BSE. If the bulk Earth, indeed, had an EH-like composition, then the isotopically heavy composition of the BSE must reflect the removal of isotopically light Sn from the BSE.

Tin plots below the volatile trend estimated from the moderately volatile element content of the BSE, which is interpreted as the fractionation of Sn into the core ([Palme et al., 2014](#)). Given the geochemistry of Sn, some possible mechanisms that would explain an enrichment of heavy Sn isotopes in the BSE include i) the segregation of metallic Sn into the core, ii) removal of chalcophile Sn into a sulphide matte ([O'Neill, 1991](#); [Wood and Halliday, 2005](#); [Savage et al., 2015](#)), iii) loss of isotopically light Sn from Earth or its precursor bodies through impact driven volatile loss ([Hin et al., 2017](#)), or iv) enrichment of isotopically light chondrules following chondrule-rich accretion of the Earth's precursors ([Johansen et al., 2015](#)).

Synchrotron (nuclear resonant inelastic X-ray scattering) experiments have shown that significant Sn isotope fractionation is expected to accompany changes in oxidation state, e.g., $\text{Sn}^{\text{IV}}\text{O}_2$ – Sn^0 (metallic) or $\text{Sn}^{\text{IV}}\text{O}_2$ – $\text{Sn}^{\text{II}}\text{O}$, even at high temperatures (≥ 1000 K; [Polyakov et al., 2005](#); [Dauphas et al., 2018](#)). This has been borne out by analyses of igneous terrestrial rocks, which have revealed significant Sn isotope fractionation relating to Sn coordination during igneous differentiation

(Creech et al., 2017; Badullovich et al., 2017). However, none of these relate directly to the behaviour of Sn during metal/silicate/sulphide fractionation during core formation. Based on the behaviour of other elements (e.g., Cu, Mo; Hin et al., 2013; Savage et al., 2015) and stable isotope theory (Schauble, 2004), we can expect that metals and sulphides should be enriched in the lighter isotopes of Sn compared to silicates in equilibrium. Thus, removal of Sn into either of those phases during formation of the core or a sulphide matte could result in the observed isotopic shift from an enstatite chondrite-like starting composition. Similarly, evaporative loss of Sn would also deplete the silicate Earth in the lighter isotopes of Sn. Therefore, any of the mechanisms discussed above would be expected to leave the BSE with depleted Sn abundances and enriched in the heavy Sn isotopes.

Given the siderophile and chalcophile behaviour of Sn, a significant fraction of Earth's Sn may have been segregated into the core or a sulphide matte (O'Neill, 1991), or lost through volatility during planetary processes (i.e. impacts). Further experimental information on the isotopic and elemental partitioning of Sn between metals, sulphides and silicates, calibration of isotopic fractionation of Sn during evaporation under various physical conditions (P, T, fO_2 , composition), and analyses of individual chondrules from carbonaceous chondrites will assist with discerning which amongst these hypotheses is most likely.

5. Conclusions

We have characterised the Sn stable isotopic composition of a range of primitive chondrite samples from the major chondrite groups. Our data reveal significant ($> 2\%$) mass-dependent Sn isotope variations amongst chondrite meteorite samples. We find that Sn and Zn abundances covary across all chondrite groups. In the ordinary chondrites, where we have data from the same sample powders, Sn and Zn isotope data are also correlated. These data suggest that both Sn and Zn isotopes were affected by a common process. Neither isotope systems shows a clear isotopic effect of petrologic type (i.e., metamorphic grade, aqueous alteration), although greater scatter is observed in the higher petrologic types. Given the differences in geochemical behaviour between these elements, the isotopic fractionations are likely related to their similar volatility. The large variations within the ordinary chondrites reflect changing compositions or populations of chondrules or the solar nebula with time. The bulk silicate Earth composition ($\delta^{122/118}\text{Sn} = 0.49 \pm 0.11\%$) overlaps with carbonaceous chondrites ($\delta^{122/118}\text{Sn} = 0.43 \pm 0.12\%$), while enstatite chondrites are relatively isotopically light ($\delta^{122/118}\text{Sn} = 0.18 \pm 0.21\%$). An enstatite chondrite-like Earth would thus require removal of isotopically light Sn from the silicate Earth through either sequestration into metals or sulphides during planetary differentiation or evaporative loss of volatiles from the primordial Earth or its precursors.

Acknowledgments

The authors thank the technical staff at IPGP for supporting the analytical work, and N. Badullovich for assistance with lab work. We also thank A. McCoy-West and two anonymous reviewers for their detailed and constructive feedback on this manuscript, and Don Porcelli for his efficient editorial handling of this manuscript. F.M. acknowledges funding from the European Research Council [ERC Starting grant agreement 637503-Pristine] to as well as the financial support of the UnivEarthS Labex program at Sorbonne Paris Cité [ANR-10-LABX-0023 and ANR-11-IDEX-0005-02] and a chaire d'excellence ANR-Idex Sorbonne Paris Cité. Parts of this work were supported by IPGP multidisciplinary program PARI, and by Region Île-de-France (SESAME grant no. 12015908).

Appendix A. Supplementary data

Supplementary data to this article can be found online at <https://doi.org/10.1016/j.chemgeo.2019.02.028>.

doi.org/10.1016/j.chemgeo.2019.02.028.

References

- Albarède, F., 2009. Volatile accretion history of the terrestrial planets and dynamic implications. *Nature* 461 (7268), 1227–1233. <https://doi.org/10.1038/nature08477>.
- Anders, E., 1968. Chemical processes in the early solar system, as inferred from meteorites. *Accounts of Chemical Research* 1 (10), 289–298. <https://doi.org/10.1021/ar50010a001>.
- Badullovich, N., Moynier, F., Creech, J., Teng, F.-Z., Sossi, P., 2017. Tin isotopic fractionation during igneous differentiation and Earth's mantle composition. *Geochemical Perspectives Letters* 5, 24–28. <https://doi.org/10.7185/geochemlet.1741>.
- Baedecker, P.A., Wasson, J.T., 1975. Elemental fractionations among enstatite chondrites. *Geochimica et Cosmochimica Acta* 39 (5), 735–765. [https://doi.org/10.1016/0016-7037\(75\)90013-7](https://doi.org/10.1016/0016-7037(75)90013-7).
- Barrat, J.A., Zanda, B., Moynier, F., Bollinger, C., Liorzou, C., Bayon, G., 2012. Geochemistry of CI chondrites: major and trace elements, and Cu and Zn isotopes. *Geochimica et Cosmochimica Acta* 83, 79–92. <https://doi.org/10.1016/j.gca.2011.12.011>.
- Biswas, S., Walsh, T.M., Bart, G., Lipschutz, M.E., 1980. Thermal metamorphism of primitive meteorites-XI. The enstatite meteorites: origin and evolution of a parent body. *Geochimica et Cosmochimica Acta* 44, 2097–2110.
- Bollard, J., Connelly, J.N., Whitehouse, M.J., Pringle, E.A., Bonal, L., Jørgensen, J.K., Nordlund, Å., Moynier, F., Bizzarro, M., 2017. Early formation of planetary building blocks inferred from Pb isotopic ages of chondrules. *Science Advances* 3 (8), e1700407. <https://doi.org/10.1126/sciadv.1700407>.
- Bourdon, B., Fitoussi, C., Wang, X., 2017. Isotope Fractionation During Partial Condensation. *Goldschmidt 2017*, Paris, France.
- Boyce, J.W., Treiman, A.H., Guan, Y., Ma, C., Eiler, J.M., Gross, J., Greenwood, J.P., Stolper, E.M., 2015. The chlorine isotope fingerprint of the lunar magma ocean. *Science Advances* 1 (8), e1500380. <https://doi.org/10.1126/sciadv.1500380>.
- Braukmüller, N., Wombacher, F., Hezel, D.C., Escoube, R., Münker, C., 2018. The chemical composition of carbonaceous chondrites: implications for volatile element depletion, complementarity and alteration. *Geochimica et Cosmochimica Acta* 239, 17–48. <https://doi.org/10.1016/j.gca.2018.07.023>.
- Brearley, A., 2014. Nebular versus parent body processing. In: Holland, H.D., Turekian, K.K. (Eds.), *Treatise on Geochemistry*, 2nd ed. vol. 1. Elsevier, pp. 309–334.
- Chen, H., Savage, P.S., Teng, F.-Z., Helz, R.T., Moynier, F., 2013. Zinc isotope fractionation during magmatic differentiation and the isotopic composition of the bulk Earth. *Earth and Planetary Science Letters* 369–370, 34–42. <https://doi.org/10.1016/j.epsl.2013.02.037>.
- Clayton, R.N., Mayeda, T.K., 1999. Oxygen isotope studies of carbonaceous chondrites. *Geochimica et Cosmochimica Acta* 63 (13), 2089–2104. [https://doi.org/10.1016/S0016-7037\(99\)00090-3](https://doi.org/10.1016/S0016-7037(99)00090-3).
- Clayton, R.N., Mayeda, T.K., Rubin, A.E., 1984. Oxygen isotopic compositions of enstatite chondrites and aubrites. *Journal of Geophysical Research: Solid Earth* 89 (S01), C245–C249. <https://doi.org/10.1029/JB089iS01p0C245>.
- Creech, J., Paul, B., 2015. *IsoSpike*: improved double-spike deconvolution software. *Geostandards and Geoanalytical Research* 39, 7–15. <https://doi.org/10.1111/j.1751-908X.2014.00276.x>.
- Creech, J.B., Moynier, F., Badullovich, N., 2017, May, May. Tin stable isotope analysis of geological materials by double-spike MC-ICPMS. *Chemical Geology* 457, 61–67. <https://doi.org/10.1016/j.chemgeo.2017.03.013>.
- Dauphas, N., Hu, M.Y., Baker, E.M., Hu, J., Tissot, F.L.H., Alp, E.E., Roskosz, M., Zhao, J., Bi, W., Liu, J., Lin, J.-F., Nie, N.X., Heard, A., 2018. *SciPhon*: a data analysis software for nuclear resonant inelastic X-ray scattering with applications to Fe, Kr, Sn, Eu and Dy. *Journal of Synchrotron Radiation* 25 (5), 1581–1599. <https://doi.org/10.1107/S1600577518009487>.
- de Laeter, J.R., Jeffery, P.M., 1965. The isotopic composition of terrestrial and meteoritic tin. *Journal of Geophysical Research* 70 (12), 2895–2903. <https://doi.org/10.1029/JZ070i012p02895>.
- de Laeter, J.R., Jeffery, P.M., 1967. Tin: its isotopic and elemental abundance. *Geochimica et Cosmochimica Acta* 31 (6), 969–985. [https://doi.org/10.1016/0016-7037\(67\)90074-9](https://doi.org/10.1016/0016-7037(67)90074-9).
- de Laeter, J.R., McCulloch, M.T., Rosman, K.J.R., 1974. Mass spectrometric isotope dilution analyses of tin in stony meteorites and standard rocks. *Earth and Planetary Science Letters* 22 (3), 226–232. [https://doi.org/10.1016/0012-821X\(74\)90085-5](https://doi.org/10.1016/0012-821X(74)90085-5).
- Defouilly, C., Cartigny, P., Assayag, N., Moynier, F., Barrat, J.A., 2016. High-precision sulfur isotope composition of enstatite meteorites and implications of the formation and evolution of their parent bodies. *Geochimica et Cosmochimica Acta* 172, 393–409. <https://doi.org/10.1016/j.gca.2015.10.009>.
- Friedrich, J.M., Perrotta, G.C., Kimura, M., 2014. Compositions, geochemistry, and shock histories of recrystallized LL chondrites. *Geochimica et Cosmochimica Acta* 139, 83–97. <https://doi.org/10.1016/j.gca.2014.04.044>.
- Friedrich, J.M., Wang, M.-S., Lipschutz, M.E., 2002. Comparison of the trace element composition of Tagish Lake with other primitive carbonaceous chondrites. *Meteoritics & Planetary Science* 37 (5), 677–686. <https://doi.org/10.1111/j.1945-5100.2002.tb00847.x>.
- Friedrich, J.M., Wang, M.-S., Lipschutz, M.E., 2003. Chemical studies of L chondrites. V: compositional patterns for 49 trace elements in 14 LL4-6 and 7 LL4-6 falls. *Geochimica et Cosmochimica Acta* 67 (13), 2467–2479. [https://doi.org/10.1016/S0016-7037\(03\)00024-3](https://doi.org/10.1016/S0016-7037(03)00024-3).
- Gao, X., Thiemens, M.H., 1991. Systematic study of sulfur isotopic composition in iron meteorites and the occurrence of excess ^{33}S and ^{36}S . *Geochimica et Cosmochimica*

- Acta 55 (9), 2671–2679. [https://doi.org/10.1016/0016-7037\(91\)90381-E](https://doi.org/10.1016/0016-7037(91)90381-E).
- Halliday, A.N., Porcelli, D., 2001. In search of lost planets – the paleocosmochemistry of the inner solar system. *Earth and Planetary Science Letters* 192 (4), 545–559. [https://doi.org/10.1016/S0016-7037\(01\)00479-4](https://doi.org/10.1016/S0016-7037(01)00479-4).
- Hamaguchi, H., Onuma, N., Hiraio, Y., Yokoyama, H., Bando, S., Furukawa, M., 1969. The abundances of arsenic, tin and antimony in chondritic meteorites. *Geochimica et Cosmochimica Acta* 33 (4), 507–518. [https://doi.org/10.1016/0016-7037\(69\)90130-6](https://doi.org/10.1016/0016-7037(69)90130-6).
- Hin, R.C., Burkhardt, C., Schmidt, M.W., Bourdon, B., Kleine, T., 2013. Experimental evidence for Mo isotope fractionation between metal and silicate liquids. *Earth and Planetary Science Letters* 379, 38–48. <https://doi.org/10.1016/j.epsl.2013.08.003>.
- Hin, R.C., Coath, C.D., Carter, P.J., Nimmo, F., Lai, Y.-J., Pogge von Strandmann, P.A.E., Willbold, M., Leinhardt, Z.M., Walter, M.J., Elliott, T., 2017. Magnesium isotope evidence that accretional vapour loss shapes planetary compositions. *Nature* 549 (7673), 511–515. <https://doi.org/10.1038/nature23899>.
- Javoy, M., 1995. The integral enstatite chondrite model of the Earth. *Geophysical Research Letters* 22 (16), 2219–2222.
- Jochum, K.P., Hofmann, A.W., Seufert, H.M., 1993. Tin in mantle-derived rocks: constraints on Earth evolution. *Geochimica et Cosmochimica Acta* 57 (15), 3585–3595. [https://doi.org/10.1016/0016-7037\(93\)90141-1](https://doi.org/10.1016/0016-7037(93)90141-1).
- Johansen, A., Low, M.-M.M., Lacerda, P., Bizzarro, M., 2015. Growth of asteroids, planetary embryos, and Kuiper belt objects by chondrule accretion. *Science Advances* 1 (3), e1500109. <https://doi.org/10.1126/sciadv.1500109>.
- Jones, R.H., 2012. Petrographic constraints on the diversity of chondrule reservoirs in the protoplanetary disk. *Meteoritics & Planetary Science* 47 (7), 1176–1190. <https://doi.org/10.1111/j.1945-5100.2011.01327.x>.
- Kato, C., Moynier, F., 2017a. Gallium isotopic evidence for extensive volatile loss from the Moon during its formation. *Science Advances* 3 (7), e1700571. <https://doi.org/10.1126/sciadv.1700571>.
- Kato, C., Moynier, F., 2017b. Gallium isotopic evidence for the fate of moderately volatile elements in planetary bodies and refractory inclusions. *Earth and Planetary Science Letters* 479, 330–339. <https://doi.org/10.1016/j.epsl.2017.09.028>.
- Kato, C., Moynier, F., Valdes, M.C., Dhaliwal, J.K., Day, J.M.D., 2015. Extensive volatile loss during formation and differentiation of the Moon. *Nature Communications* 6, 7617 EP. <https://doi.org/10.1038/ncomms8617>.
- Keil, K., 1989. Enstatite meteorites and their parent bodies. *Meteoritics* 24 (4), 195–208. <https://doi.org/10.1111/j.1945-5100.1989.tb00694.x>.
- Kong, P., Mori, T., Ebihara, M., 1997. Compositional continuity of enstatite chondrites and implications for heterogeneous accretion of the enstatite chondrite parent body. *Geochimica et Cosmochimica Acta* 61 (22), 4895–4914. [https://doi.org/10.1016/S0016-7037\(97\)00278-0](https://doi.org/10.1016/S0016-7037(97)00278-0).
- Larimer, J.W., Anders, E., 1967. Chemical fractionations in meteorites—II. Abundance patterns and their interpretation. *Geochimica et Cosmochimica Acta* 31 (8), 1239–1270. [https://doi.org/10.1016/S0016-7037\(67\)80014-0](https://doi.org/10.1016/S0016-7037(67)80014-0).
- Lin, Y., Goresy, A.E., 2002. A comparative study of opaque phases in Qingzhen (EH3) and MacAlpine Hills 88136 (EL3): representatives of EH and EL parent bodies. *Meteoritics & Planetary Science* 37 (4), 577–599. <https://doi.org/10.1111/j.1945-5100.2002.tb00840.x>.
- Lodders, K., 2003. Solar system abundances and condensation temperatures of the elements. *The Astrophysical Journal* 591 (2), 1220. <https://doi.org/10.1086/375492>.
- Loss, R., Rosman, K., de Laeter, J., 1990. The isotopic composition of zinc, palladium, silver, cadmium, tin, and tellurium in acid-etched residues of the Allende meteorite. *Geochimica et Cosmochimica Acta* 54 (12), 3525–3536. [https://doi.org/10.1016/0016-7037\(90\)90302-2](https://doi.org/10.1016/0016-7037(90)90302-2).
- Luck, J.-M., Othman, D.B., Albarède, F., 2005. Zn and Cu isotopic variations in chondrites and iron meteorites: early solar nebula reservoirs and parent-body processes. *Geochimica et Cosmochimica Acta* 69 (22), 5351–5363. <https://doi.org/10.1016/j.gca.2005.06.018>.
- Luck, J.M., Othman, D.B., Barrat, J.A., Albarède, F., 2003. Coupled ^{63}Cu and ^{16}O excesses in chondrites. *Geochimica et Cosmochimica Acta* 67 (1), 143–151.
- Mittlefehldt, D.W., Lindstrom, M.M., 1991. Generation of abnormal trace element abundances in Antarctic eucrites by weathering processes. *Geochimica et Cosmochimica Acta* 55 (1), 77–87.
- Morgan, J.W., Higuchi, H., Takahashi, H., Hertogen, J., 1978. A “chondritic” eucrite parent body: inference from trace elements. *Geochimica et Cosmochimica Acta* 42 (1), 27–38. [https://doi.org/10.1016/0016-7037\(78\)90213-2](https://doi.org/10.1016/0016-7037(78)90213-2).
- Mougel, B., Moynier, F., Göpel, C., Koerber, C., 2017. Chromium isotope evidence in ejecta deposits for the nature of Paleoproterozoic impactors. *Earth and Planetary Science Letters* 460, 105–111. <https://doi.org/10.1016/j.epsl.2016.12.008>.
- Moynier, F., Paniello, R.C., Gounelle, M., Albarède, F., Beck, P., Podosek, F., Zanda, B., 2011. Nature of volatile depletion and genetic relationships in enstatite chondrites and aubrites inferred from Zn isotopes. *Geochimica et Cosmochimica Acta* 75 (1), 297–307.
- Norris, C.A., Wood, B.J., 2017. Earth's volatile contents established by melting and vaporization. *Nature* 549 (7673), 507–510. <https://doi.org/10.1038/nature23645>.
- O'Neill, H.S.C., 1991. The origin of the moon and the early history of the earth—a chemical model. Part I: the moon. *Geochimica et Cosmochimica Acta* 55 (4), 1135–1157. [https://doi.org/10.1016/0016-7037\(91\)90168-5](https://doi.org/10.1016/0016-7037(91)90168-5).
- O'Neill, H.S.C., Palme, H., 2008. Collisional erosion and the non-chondritic composition of the terrestrial planets. *Philosophical Transactions of the Royal Society of London A: Mathematical, Physical and Engineering Sciences* 366 (1883), 4205–4238. <https://doi.org/10.1098/rsta.2008.0111>.
- Palme, H., Lodders, K., Jones, A., 2014. Solar system abundances of the elements. In: Holland, H.D., Turekian, K.K. (Eds.), *Treatise on Geochemistry*, 2nd ed. vol. 2. Elsevier, pp. 15–36.
- Paniello, R.C., 2013. Volatilization of Extraterrestrial Materials as Determined by Zinc Isotopic Analysis. Ph.D. thesis. Washington University in St. Louis.
- Paniello, R.C., Moynier, F., Beck, P., Barrat, J.-A., Podosek, F.A., Pichat, S., 2012. Zinc isotopes in HEDs: clues to the formation of 4-Vesta, and the unique composition of Pecora Escarpment 82502. *Geochimica et Cosmochimica Acta* 86, 76–87. <https://doi.org/10.1016/j.gca.2012.01.045>.
- Patten, C., Barnes, S.-J., Mathez, E.A., Jenner, F.E., 2013. Partition coefficients of chalcophile elements between sulfide and silicate melts and the early crystallization history of sulfide liquid: LA-ICP-MS analysis of MORB sulfide droplets. *Chemical Geology* 358, 170–188. <https://doi.org/10.1016/j.chemgeo.2013.08.040>.
- Poitrasson, F., Halliday, A.N., Lee, D.-C., Levasseur, S., Teutsch, N., 2004. Iron isotope differences between Earth, Moon, Mars and Vesta as possible records of contrasted accretion mechanisms. *Earth and Planetary Science Letters* 223 (3–4), 253–266. <https://doi.org/10.1016/j.epsl.2004.04.032>.
- Polyakov, V.B., Mineev, S.D., Clayton, R.N., Hu, G., Mineev, K.S., 2005. Determination of tin equilibrium isotope fractionation factors from synchrotron radiation experiments. *Geochimica et Cosmochimica Acta* 69 (23), 5531–5536. <https://doi.org/10.1016/j.gca.2005.07.010>.
- Pringle, E.A., Moynier, F., 2017. Rubidium isotopic composition of the Earth, meteorites, and the Moon: evidence for the origin of volatile loss during planetary accretion. *Earth and Planetary Science Letters* 473, 62–70. <https://doi.org/10.1016/j.epsl.2017.05.033>.
- Pringle, E.A., Moynier, F., Beck, P., Paniello, R., Hezel, D.C., 2017. The origin of volatile element depletion in early solar system material: clues from Zn isotopes in chondrites. *Earth and Planetary Science Letters* 468, 62–71. <https://doi.org/10.1016/j.epsl.2017.04.002>.
- Pringle, E.A., Moynier, F., Savage, P.S., Badro, J., Barrat, J.-A., 2014. Silicon isotopes in angrites and volatile loss in planetesimals. *Proceedings of the National Academy of Sciences* 111 (48), 17029–17032. <https://doi.org/10.1073/pnas.1418889111>.
- Regelung, M., Elliott, T., Coath, C.D., 2008. Nickel isotope heterogeneity in the early solar system. *Earth and Planetary Science Letters* 272 (1–2), 330–338. <https://doi.org/10.1016/j.epsl.2008.05.001>.
- Ringwood, A., 1966. Chemical evolution of the terrestrial planets. *Geochimica et Cosmochimica Acta* 30 (1), 41–104. [https://doi.org/10.1016/0016-7037\(66\)90090-1](https://doi.org/10.1016/0016-7037(66)90090-1).
- Savage, P., Moynier, F., Chen, H., Shofner, G., Siebert, J., Badro, J., Puchtel, I., 2015. Copper isotope evidence for large-scale sulphide fractionation during Earth's differentiation. *Geochemical Perspectives Letters* 1 (1), 53–64. <https://doi.org/10.7185/geochemlet.1506>.
- Schauble, E.A., 2004. Applying stable isotope fractionation theory to new systems. *Reviews in Mineralogy and Geochemistry* 55 (1), 65–111. <https://doi.org/10.2138/gsrmg.55.1.65>.
- Schediwiy, S., Rosman, K., de Laeter, J., 2006. Mar. Mar. Isotope fractionation of cadmium in lunar material. *Earth and Planetary Science Letters* 243 (3–4), 326–335. <https://doi.org/10.1016/j.epsl.2006.01.007>.
- Schiller, M., Bizzarro, M., Fernandes, V.A., 2018. Isotopic evolution of the protoplanetary disk and the building blocks of Earth and the Moon. *Nature* 555 (7697), 507–510. <https://doi.org/10.1038/nature25990>.
- Schönbächler, M., Carlson, R., Horan, M., Mock, T., Hauri, E., 2008. Nov. Nov. Silver isotope variations in chondrites: volatile depletion and the initial ^{107}Pd abundance of the solar system. *Geochimica et Cosmochimica Acta* 72 (21), 5330–5341. <https://doi.org/10.1016/j.gca.2008.07.032>.
- Scott, E.R.D., Krot, A.N., 2014. Chondrites and their components. In: Holland, H.D., Turekian, K.K. (Eds.), *Treatise on Geochemistry*, 2nd ed. 1. Elsevier, pp. 65–137.
- Sears, D.W., Kallemeyn, G.W., Wasson, J.T., 1982. The compositional classification of chondrites: II. The enstatite chondrite groups. *Geochimica et Cosmochimica Acta* 46 (4), 597–608. [https://doi.org/10.1016/0016-7037\(82\)90161-2](https://doi.org/10.1016/0016-7037(82)90161-2).
- Sharp, Z.D., Shearer, C.K., McKeegan, K.D., Barnes, J.D., Wang, Y.Q., 2010. The chlorine isotope composition of the Moon and implications for an anhydrous mantle. *Science* 329 (5995), 1050–1053. <https://doi.org/10.1126/science.1192606>.
- Shima, M., 1964. The distribution of germanium and tin in meteorites. *Geochimica et Cosmochimica Acta* 28 (4), 517–532. [https://doi.org/10.1016/0016-7037\(64\)90122-X](https://doi.org/10.1016/0016-7037(64)90122-X).
- Sossi, P.A., Moynier, F., Zuilen, K. v., 2018. Volatile loss following cooling and accretion of the Moon revealed by chromium isotopes. *Proceedings of the National Academy of Sciences* 115 (43), 10920–10925. <https://doi.org/10.1073/pnas.1809060115>.
- Trinquier, A., Birk, J.-L., Allègre, C.J., 2007. Widespread ^{54}Cr heterogeneity in the inner solar system. *The Astrophysical Journal* 655 (2), 1179. <https://doi.org/10.1086/510360>.
- Tyburczy, J.A., Frisch, B., Ahrens, T.J., 1986. Shock-induced volatile loss from a carbonaceous chondrite: implications for planetary accretion. *Earth and Planetary Science Letters* 80 (3–4), 201–207. [https://doi.org/10.1016/0012-821X\(86\)90104-4](https://doi.org/10.1016/0012-821X(86)90104-4).
- Uesugi, M., Sekiya, M., Nakamura, T., 2010. Kinetic stability of a melted iron globule during chondrule formation. I. Non-rotating model. *Meteoritics & Planetary Science* 43 (4), 717–730. <https://doi.org/10.1111/j.1945-5100.2008.tb00680.x>.
- Vollstaedt, H., Mezger, K., Leya, I., 2016. The isotope composition of selenium in chondrites constrains the depletion mechanism of volatile elements in solar system materials. *Earth and Planetary Science Letters* 450, 372–380. <https://doi.org/10.1016/j.epsl.2016.06.052>.
- Wang, K., Jacobsen, S.B., 2016. Potassium isotopic evidence for a high-energy giant impact origin of the Moon. *Nature* 538 (7626), 487–490. <https://doi.org/10.1038/nature19341>.
- Wang, X., Amet, Q., Fitoussi, C., Bourdon, B., 2018. Tin isotope fractionation during magmatic processes and the isotope composition of the bulk silicate Earth. *Geochimica et Cosmochimica Acta* 228, 320–335. <https://doi.org/10.1016/j.gca.2018.02.014>.
- Wang, X., Fitoussi, C., Bourdon, B., Amet, Q., 2017. A new method of Sn purification and

- isotopic determination with a double-spike technique for geological and cosmochemical samples. *Journal of Analytical Atomic Spectrometry* 32 (5), 1009–1019. <https://doi.org/10.1039/C7JA00031F>.
- Wasson, J.T., Chou, C.-L., 1974. Fractionation of moderately volatile elements in ordinary chondrites. *Meteoritics* 9 (1), 69–84. <https://doi.org/10.1111/j.1945-5100.1974.tb00063.x>.
- Wasson, J.T., Kallemeyn, G.W., 1988. Compositions of chondrites. *Philosophical Transactions of the Royal Society of London. Series A, Mathematical and Physical Sciences* 325 (1587), 535–544.
- Wasson, J.T., Rubin, A.E., 2010. Metal in CR chondrites. *Geochimica et Cosmochimica Acta* 74 (7), 2212–2230. <https://doi.org/10.1016/j.gca.2010.01.014>.
- Wlotzka, F., 1993. A weathering scale for the ordinary chondrites. *Meteoritics* 28, 460.
- Wombacher, F., Rehkämper, M., Mezger, K., Bischoff, A., Münker, C., 2008. Cadmium stable isotope cosmochemistry. *Geochimica et Cosmochimica Acta* 72 (2), 646–667. <https://doi.org/10.1016/j.gca.2007.10.024>.
- Wood, B.J., Halliday, A.N., 2005. Cooling of the Earth and core formation after the giant impact. *Nature* 437 (7063), 1345.